1 QCD and the hadronic final state

1.1 Event Shapes

A recent revival of interest in the study of event shape measurements has been prompted by theoretical developments in the understanding of hadronisation or power corrections. Here, perturbative QCD calculations are extended into the region of low momentum transfers using approximations to higher-order graphs. At HERA, the Q^2 scale can be varied over four orders of magnitude enabling power corrections (proportional to $1/Q^p$, where p is the power) to be studied in detail. The data are compared to theoretical expectations for the power corrections, characterised by an effective coupling $\overline{\alpha}_0(\mu_I)$ specified at the infra-red matching scale $\mu_I \simeq 2$ GeV, and NLO pQCD calculations, determined by $\alpha_s(M_Z)$.

The Breit frame is where the exchanged gauge boson in DIS is purely space-like. Viewed in this frame, the incoming QPM quark is back-scattered with equal and opposite momentum $(Q/2)$. Event shapes have been measured in the direction of the struck quark, corresponding to the current region, which is directly analogous to one hemisphere of a purely time-like e^+e^- interaction. A series of event shape variables have been studied which have varying sensitivity to hadronisation/power corrections and are noted below. Thrust ($\tau = 1 - T_z$) and jet broadening (B) sum the longitudinal and transverse momenta, respectively, of individual particles along the photon axis. τ_c is also defined with respect to the reconstructed thrust axis, in order to compare directly with e^+e^-. Jet mass (ρ) and the C parameter sum the product of two particle momenta weighted by $1 - \cos\theta_{ij}$ and $\sin^2\theta_{ij}$, respectively. These variables are each measured in the current region of the Breit frame and are scaled by the total visible energy (E_{vis}).

Mean values of these event shapes haves been measured by ZEUS [1] which can be interpreted theoretically via

$$\langle F \rangle = \langle F \rangle^{\rm pert} + \langle F \rangle^{\rm pow}$$

where

$$\langle F \rangle^{\rm pert} = c_{1,F}(x,Q) \cdot \alpha_s(Q) + c_{2,F}(x,Q) \cdot \alpha_s^2(Q)$$

with $c_{1,F}(x,Q)$ and $c_{2,F}(x,Q)$ being calculable coefficients of pQCD determined by the DISENT NLO program with renormalisation/factorisation scales set at $\mu_R = \mu_F = Q$. The power corrections are proportional to $1/Q$ with

$$\langle F \rangle^{\rm pow} = \mathcal{M}' \frac{a_F}{Q} \frac{16\mu_I}{3\pi} \left[\overline{\alpha}_0(\mu_I) - \alpha_s(Q) - \frac{23}{6\pi} \left(\ln \frac{Q}{\mu_I} + 1.45 \right) \alpha_s^2(Q) \right].$$

Here a_F is a calculable F-dependent coefficient and $\mathcal{M}' = 2\mathcal{M}/\pi \simeq 0.95$ is a two-loop level refinement to the calculations called the Milan factor.

Using the NLO calculation plus power correction approach described above, the mean event shape values versus Q are measured. Overall, a reasonable description of the data can be achieved, although the x-dependence of variables measured with respect to the photon axis, τ and B, is not well described. The major theoretical uncertainty is that due to the renormalisation scale.

The results of two-parameter fits to the ZEUS data both including and excluding the data at low x are shown in Figure 1. The correlation of $\overline{\alpha}_0(\mu_I)$ and $\alpha_s(M_Z)$ is high and negative for $\langle \tau \rangle$ but is less for other variables. In each case, the data for the means of τ, B, τ_C, C and ρ, are described reasonably well by the theory, with a value of the universal non-perturbative parameter $\overline{\alpha}_0(\mu_I)$ of $\simeq 0.5 \pm 20\%$ and a value of $\alpha_s(M_Z)$ close to the world average. There are, however, remaining theoretical uncertainties due to uncalculated higher-order x-dependent terms which appear to be especially significant for B. In conclusion, the theoretical approach works remarkably well and ongoing refinements will generate further insight into non-perturbative QCD mechanisms in the generation of hadronic final states at high energies. This analysis is currently in the final stages of the paper process and will lead to a publication soon.

1.2 Fragmentation in DIS

something from Nick here

1.3 Azimuthal Asymmetries

In the last report we presented the first observation of an azimuthal asymmetry between the lepton scattering plane and the hadron production plane for leading hadrons in the DIS hadronic centre-of-mass. This measurement has now been extended to study the angular assymmetry between between the lepton scattering plane and the jet production plane in inclusive *(dijet?)* DIS events. This is illustrated compared to the DISENT NLO QCD calculation in figure 2 and shows clear evidence for a $\cos 2\phi$ contribution, a clear consequence of the underlying QCD.

Work is continuing [3] on the use of a neural network for the identification of quark and gluon jets in dijet events since their different helicity should yield distinct angular distrubtions and provide further insight into the QCD sub-process.

1.4 Jet Production

Our studies of jets in photon-proton collisions at HERA continue to give information on the hadronic "structure" of the photon, and UK groups continue to lead these analyses. In the last report we reported on our measurement [4] of the dynamics of three jet production with higher statistics than our previous measurement [5] and showing explicitly the effects of the colour of the incoming quarks and gluons (see figure 3) – a fundamental test of the strong interaction.

In addition we have recently published [6] precise data on dijet photoproduction at high $E_T^{\rm jet}$ including the dijet angular distributions (figure 4).

Although these angular distributions present a reassuring picture of jet photoproduction in that the dynamics are well described by QCD, there is growing evidence for a significant discrepancy in the rate of resolved photon interactions, with the data lying above the NLO QCD expectations by around 30%. We have measured cross sections differentially in $\eta^{\rm jet}$, $E_T^{\rm jet}$ and $x_\gamma^{\rm OBS}$ – the fraction of the photon's momentum entering the hard subprocess. In all cases, although the direct-photon dominated high $x_\gamma^{\rm OBS}$ region agrees well with the theory, the resolved-photon dominated low-$x_\gamma^{\rm OBS}$ region shows an excess as may be seen in figure 5. The current evidence points to the photon structure as the source of this discrepancy – ZEUS is sensitive to the photon structure in a Q^2 region above that accessible by LEP. However the cross-section as a function of the cut on the transverse energy of the sub-leading jet (figure 6) suggests that the contribution from higher order processes may still be significant.

By extending the 3-jet measurement to study the inclusive 4-jet final state we are seeking to expand our understanding of the QCD sub-process at even higher orders and together with the extension of the 3-jet measurement to lower 3-jet invariant masses we are additionally able to search for signatures of multi-parton interactions – one of the leading uncertainties in the description of the jet final state at lower transverse energies.

Our recently published results [7] on dijet production at very high invariant mass, with higher precision than previously measured, allow the search for heavy resonances and new physics. Limits on $W^\pm$ and Z^0 production in the final state have been obtained and are

$\sigma_{e^+p\to e^+Z^0X} < 5.9$ pb and $\sigma_{e^+p\to e^+W^\pm X} < 7.4$ pb respectively. Although this limit on $W^\pm$ production is weaker than we obtain using the leptonic channel (section **??**) it provides a complementary picture from the hadronic final state. Limits on the production of new heavy resonances, coupling preferentially to the photon-gluon initial state, such as technicolour pseudo-Goldstone bosons [8], have also been obtained and are shown in figure 7.

1.5 Jet substructure

(maybe move this to before the discussion of the three-jet angular distributions?)

An important aspect of the description of the QCD final state in jet production, besides the overall event topology and rate of production, is in the description of structure of the jets themselves.

To study this we have measured the topology of the jets in photoproduction using both the mean jet-shape (the fraction, with respect to a cone of radius $R = 1$, of the jet energy within a cone of radius r) and the mean subjet multiplicity (the number of subjets within the jet for a varying distance scale, $y_{\rm cut}$, used in the jet finding). The width of jets in QCD is sensitive both to the QCD coupling, α_S, and to the fragmentation of the partons in the jet due to differing colour factors of the primary parton.

Figure 8 shows the mean jet shape and subjet multiplicities for photoproduction events. The tendency for gluon initiated jets to be broader can be used to divide the sample into gluon enhanced (thick) and quark enhanced (thin) jets and to study the dynamics of the underying sub-process in more detail than possible in inclusive dijet production. Figure 9 shows the dijet angular distribution in the dijet centre-of-mass frame for samples enriched in gluon-gluon, quark-quark and gluon-quark jets. *(Claudia, in the right plot is* $\cos\theta^*$ *defined with respect to the quark, or the gluon jet?)*

In addition, by studying the behaviour of the mean jet shape as a function of the jet transverse energy (figure 10) the QCD coupling constant can be extracted in a complimentary way to that from the study the jet rates themselves. This is shown in figure 11; the values of α_s thus obtained providing a non-trivial test of the consistency of our understanding of the hadronic final state.

1.6 Virtual-photon structure

Both the behaviour of the pointlike virtual photon at high Q^2 and the hadronic structure of the low virtuality photon have been well studied. By looking at the production of dijet events as a function of the photon virtuality from very low to very high Q^2 we are additionally able to study the hadronic structure of the virtual photon.

Building on our previous analysis [9], we have made use of the higher luminosity now available to study the virtual photon structure triply differentially in photon vituality, mean dijet transverse energy squared and also $x_\gamma^{\rm OBS}$. This is illustrated in figure 14 compared to predictions using the SaS 1D [10] parametrisation of the virtual photon parton density functions.

As expected, the low $x_\gamma^{\rm OBS}$ cross-section falls faster with increasing Q^2 than the high $x_\gamma^{\rm OBS}$ cross-section and for $Q^2 > \bar{E_T}^2$, the data is well descibed by the Monte Carlo with no resolved contribution required. However, for $Q^2 < \bar{E_T}^2$, the direct contribution alone is not sufficient to describe the data and further, the low $x_\gamma^{\rm OBS}$ cross-section is not well described by the Monte Carlo at lower Q^2.

1.7 Strange hadron production

Strange particle production at HERA provides an important environment for the study of the hadron production mechanism in processes containing hadronic remnants and can yield important information of the universality of strange particle fragmentation functions.

By considering strange particle production in conjunction with the production of high E_T jets in the hadronic final state it is possible to study the dependence of the hadronization mechanism on the underlying kinematics of the perturbative QCD sub-process.

Using the large event sample now available at ZEUS we have measured [11] strange particle production both to higher precision, and more differentially that before. Figure 12 shows that the cross-section for K_S^0 production in events with at least two high transverse energy jets is reasonably well described in shape by available Monte Carlo models. Figure 13 shows that while the Λ cross-section is reasonably well described in shape, normalizing the overall Monte Carlo cross-section to that given by the K_S^0 data over estimates the rate of Λ baryon production with respect to K_S^0 hadrons for HERWIG and slightly underestimates for PYTHIA.

1.8 Inclusive Prompt Photon Photoproduction

Further progress has been made in studying photoproduction processes in which a high-E_T photon is emitted. Such photons may be produced directly as part of the QCD hard scattering subprocess, and are known as prompt photons. In a first ZEUS paper [12] the observation of such processes was first confirmed at HERA and the basic characteristics of events with a prompt photon and a counterbalancing jet were established. In a more recent paper [13] the properties of inclusive prompt photons have been studied.

High energy photon production can be described as a sum of direct processes, dominated by the elastic scattering of the incoming photon off a quark in the proton, and resolved processes, in which the incoming photon is a source of partons which subsequently scatter. A source of photons which it is desirable to minimise comes from dijet processes in which a final state quark hard-radiates a photon, referred to radiative events. The requirement that the final-state photon be relatively isolated from other final-state particles reduces the radiative contribution and also neutral-meson backgrounds. The latter are finally subtracted off by means of signal-shape properties in the ZEUS barrel calorimeter.

Figure 15a shows the transverse energy of the prompt photons observed by ZEUS, compared with various theoretical predictions, for photon pseudorapidities in the range plotted in figure 15b. Here, the pseudorapidity η^γ of the photon is plotted for photons in the E_T range 5-10 GeV. LG denotes the NLO theory of Gordon; K&Z denotes that of Krawczyk and Zembruski. The two figures show that the transverse energy is well predicted on average by most of the theories, although HERWIG is a little low. However the observed pseudorapidity of the photons is higher than all the theories in the rear region, although the statistical significance is not large. This may requires further theoretical input.

We plan to improve these measurements by using the considerably increased statistics that are now becoming available, and by improving our techniques to include photons in the forward and rear calorimeters as well as the barrel. At the same time, we are engaged in an analysis of the intrinsic k_T of partons in the proton, which can be probed by means of the kinematics of events with a prompt photon and a jet. This is in response to a number of prompt photon measurements mainly from Fermilab, which seem to imply surprisingly large values of this quantity. We are currently extending this analysis to include the study of prompt photons in DIS events.

This entire area of study will be further enhanced by the very much improved luminosities available after the HERA upgrade.

References

[1] R. Waugh, Glasgow University PhD Thesis (1999); G. McCance, "Event Shapes at HERA", Moriond Proceedings (in preparation *(still?)*); G. McCance, Glasgow University Ph.D. Thesis (2000?)

[2] N.Brook and I.Skillicorn; Phys. Lett. **B497** (2001) 55; Phys. Lett. **B479** (2000) 173.

[3] E.Rodrigues; University of Bristol PhD Thesis (in preparation).

[4] E.A.Heaphy, *Three-jet Production at HERA*, Durham Workshop on Collider Physics, (Sept. 1999) *(published, proper citation)*; University College London PhD Thesis (2001).

[5] ZEUS Collaboration, J. Breitweg et al., Phys. Lett. B 443 (1998) 394-408.

[6] ZEUS Collaboration; *Dijet photoproduction and photon structure* to be published in Eur. Phys. J.(?).

[7] ZEUS Collaboration; *High mass dijets in photoproduction* to be published in Phys. Lett. **B**

[8] S.Weinberg; Phys. Rev. **D19** (1979) 1277; L.Susskind; Phys. Rev. **D20** (1979) 2619;

[9] ZEUS Collaboration; *virtual photon structure* Eur. Phys. J. (?); N.MacDonald, Glasgow University PhD Thesis (1999?).

[10] T.Sjöstrand and G.A.Schuler; Z. Phys. **C68** (1995) 607.

[11] S.Boogert; University of Oxford PhD Thesis (in preparation); Photon 2001 proceedings.

[12] ZEUS Collaboration, J. Breitweg et al., Phys. Lett. B 413 (1997) 201.

[13] ZEUS Collaboration, J. Breitweg et al., Phys. Lett. B 472 (2000) 175.

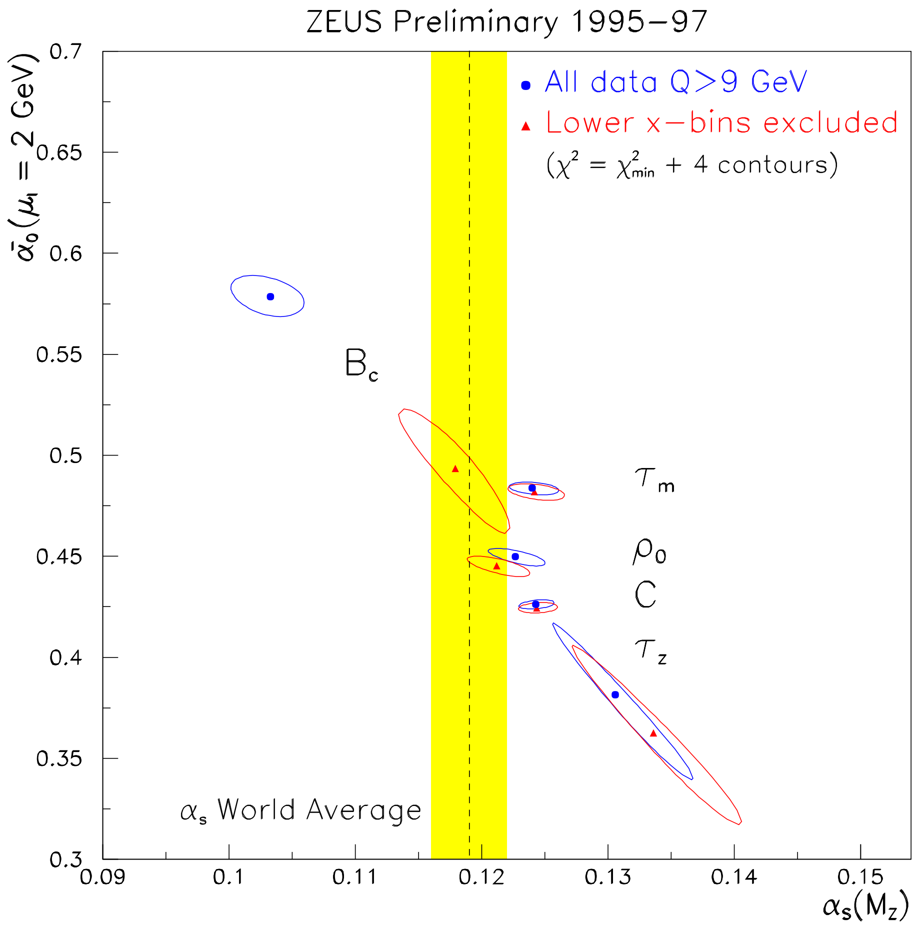

Figure 1: ZEUS preliminary contour plot of two-parameter fits of $\overline{\alpha}_0(\mu_I)$ and $\alpha_s(M_Z)$ to mean event shape variables. Two σ stat contours for fits both including and excluding the lower x data for τ, B, τ_C, ρ and C parameters are indicated.

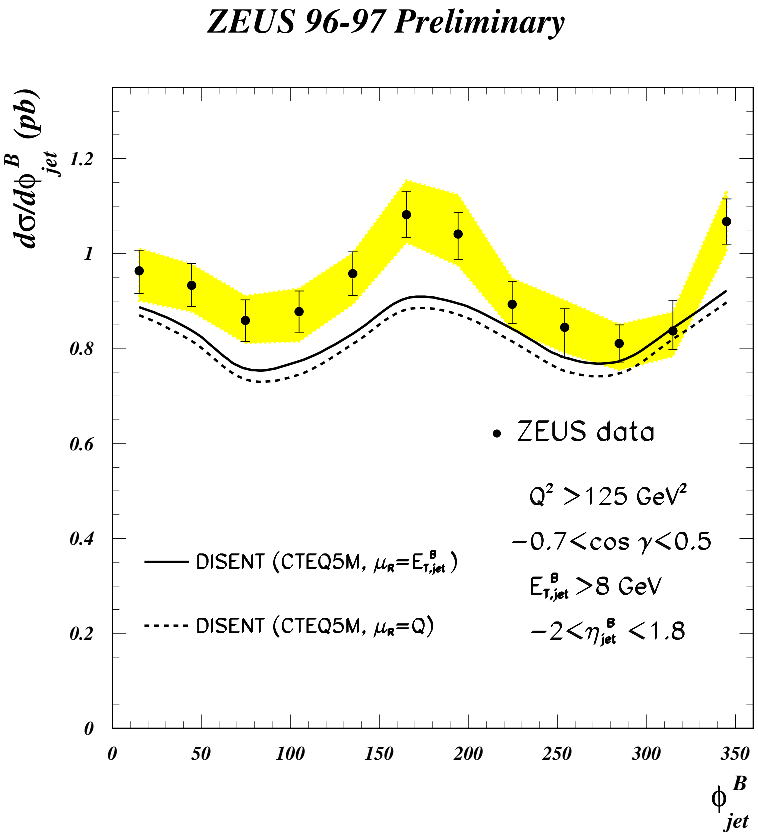

Figure 2: ZEUS preliminary jet cross section versus angle $\phi^B_{\rm jet}$ in the Breit frame in DIS compared to the DISENT NLO QCD calculation. The shaded area indicates the hadronic energy-scale uncertainty.

ZEUS 1996 -1997 Preliminary

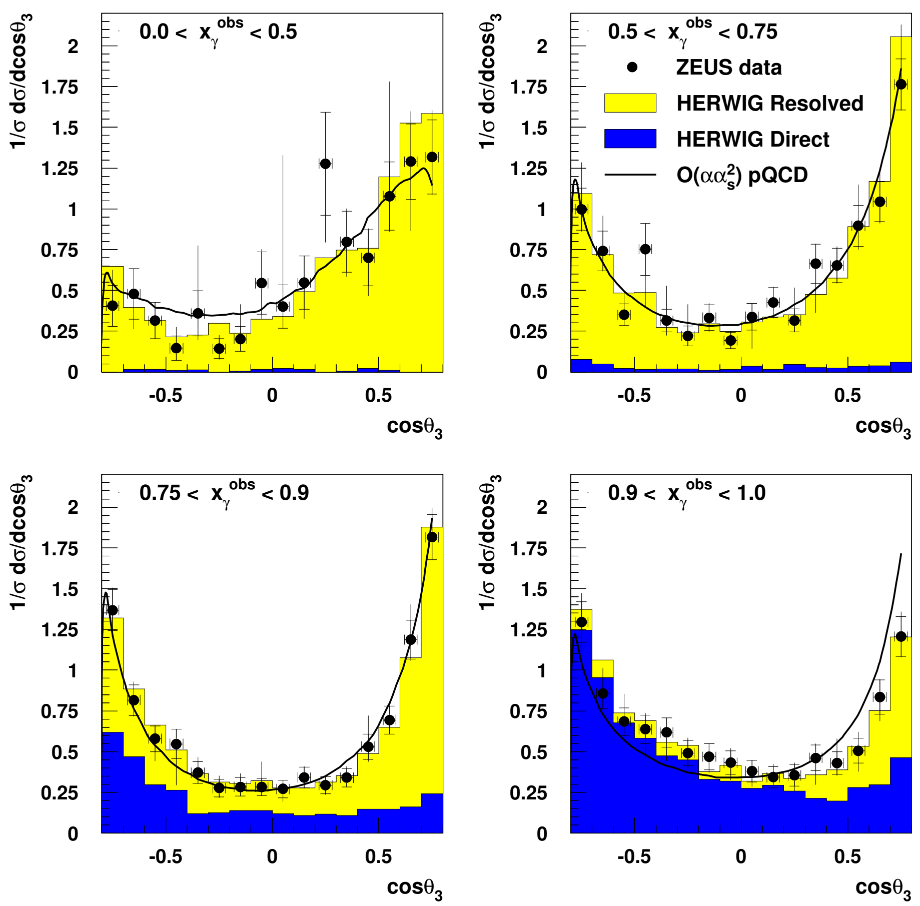

Figure 3: ZEUS preliminary three jet cross sections. Leading-log (LL) Monte Carlo resolved-photon processes are shown by light shading, and LL Monte Carlo direct by dark shading. The $\mathcal{O}(\alpha\alpha_s^2)$ tree-level calculation is shown as the curve.

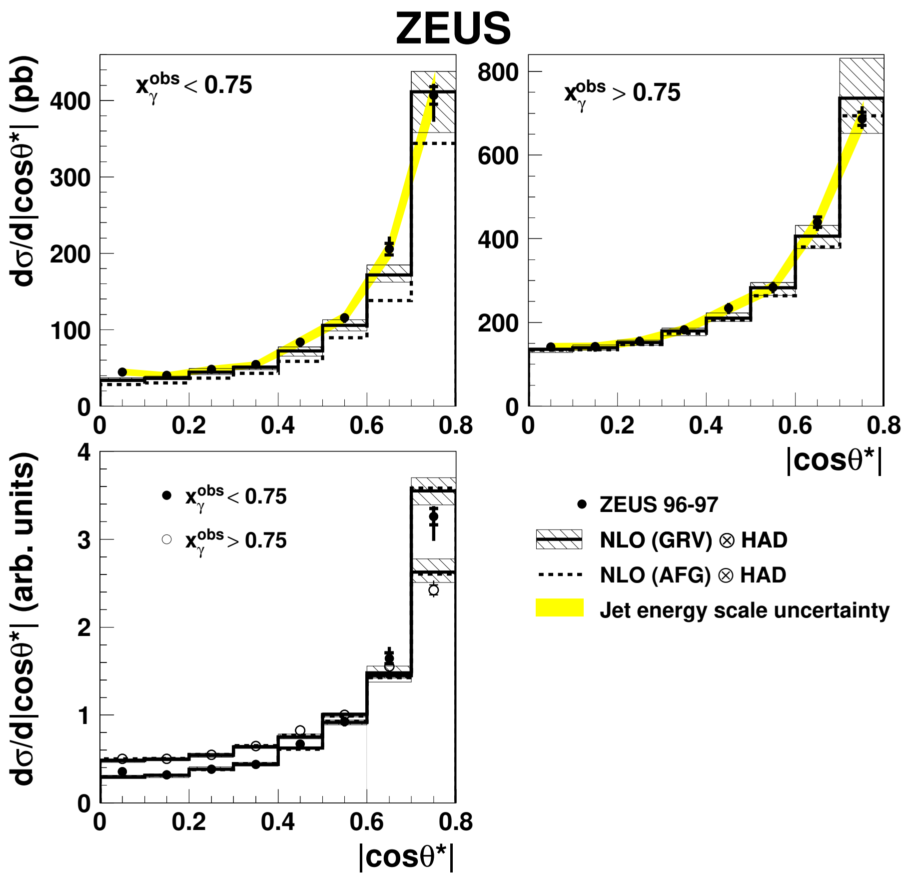

Figure 4: ZEUS jet cross sections compared to the NLO QCD calculation of Frixione and Ridolfi. The shaded areas for the data the theory prediction indicate the hadronic energy-scale uncertainty and the theoretical uncertainty respectively.

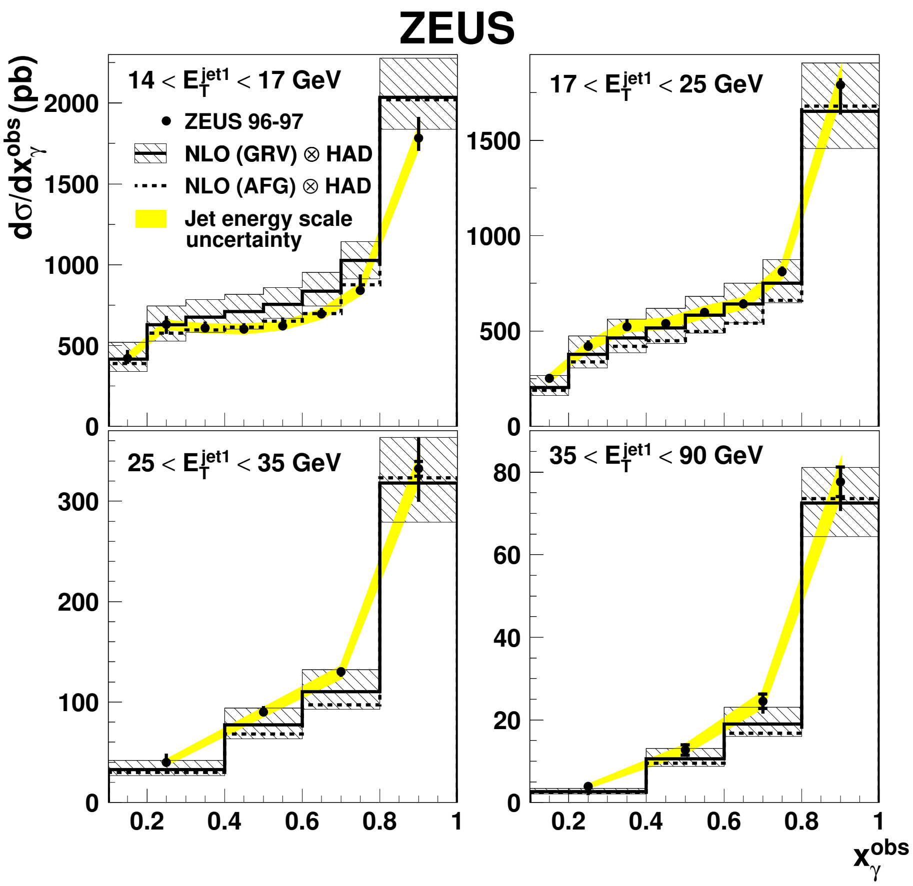

Figure 5: ZEUS jet cross sections compared to the NLO QCD calculation of Frixione and Ridolfi. The shaded areas for the data the theory prediction indicate the hadronic energy-scale uncertainty and the theoretical uncertainty respectively.

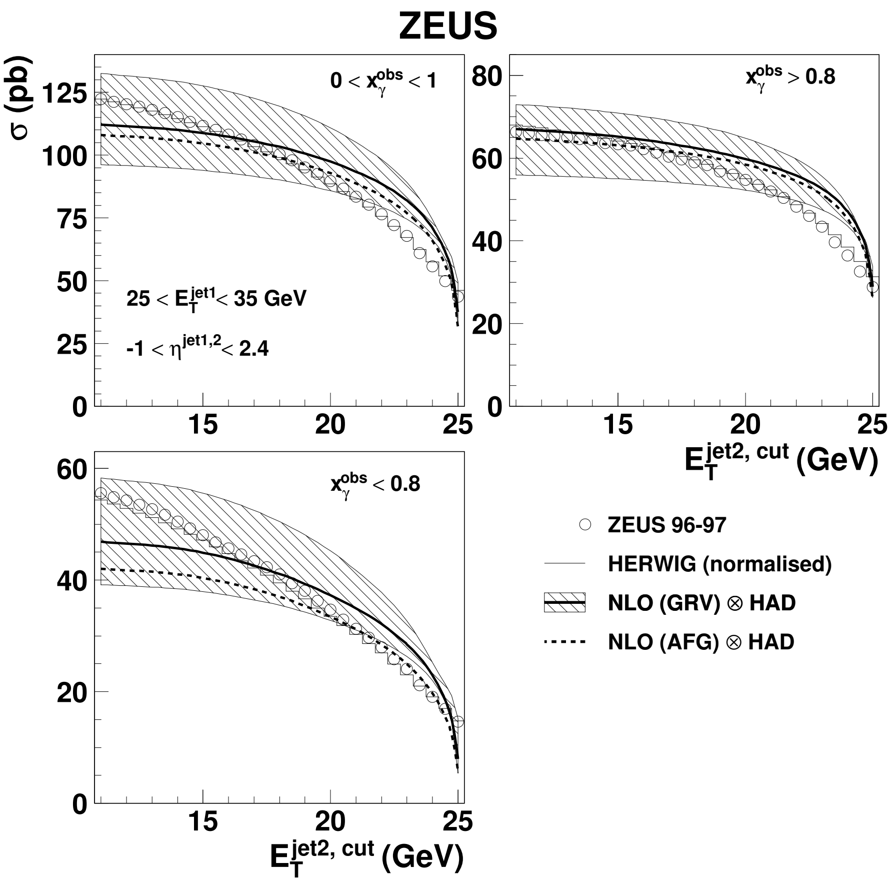

Figure 6: Total ZEUS dijet cross-sections for differing E_T cut on the sub-leading jet compared to HERWIG and the NLO QCD calculation of Frixione and Ridolfi. The shaded area indicates the NLO renormalisation scale uncertainty.

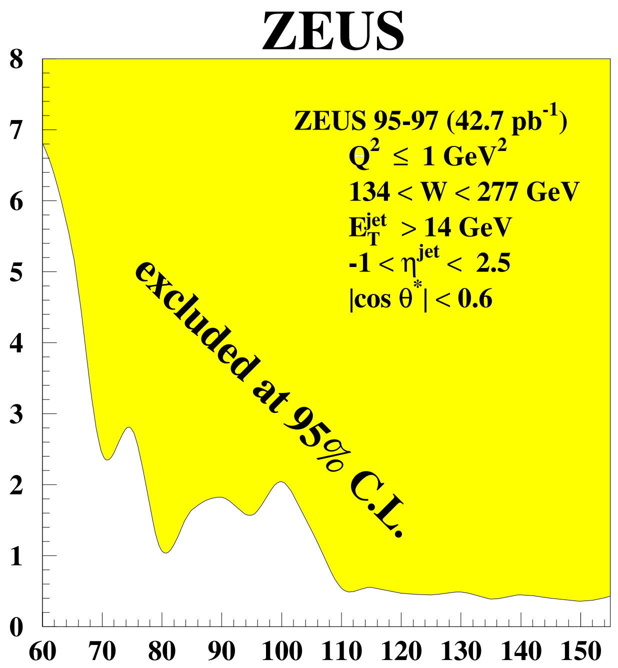

Figure 7: ZEUS excluded region of cross-section times branching ratio for new heavy resonances, $\mathcal{P}$, coupling preferentially to the photon-gluon initial state in the mass region 60< $M_{\mathcal{P}}$ <149 GeV.

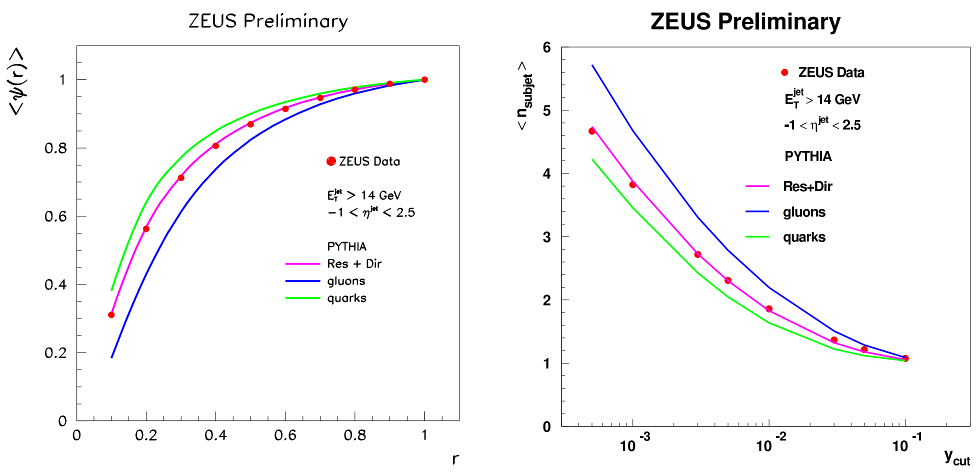

Figure 8: ZEUS preliminary results on the mean jet shape (left) and mean subjet multiplicity (right) compared to PYTHIA. For PYTHIA, both quark and gluon jets are also shown separately.

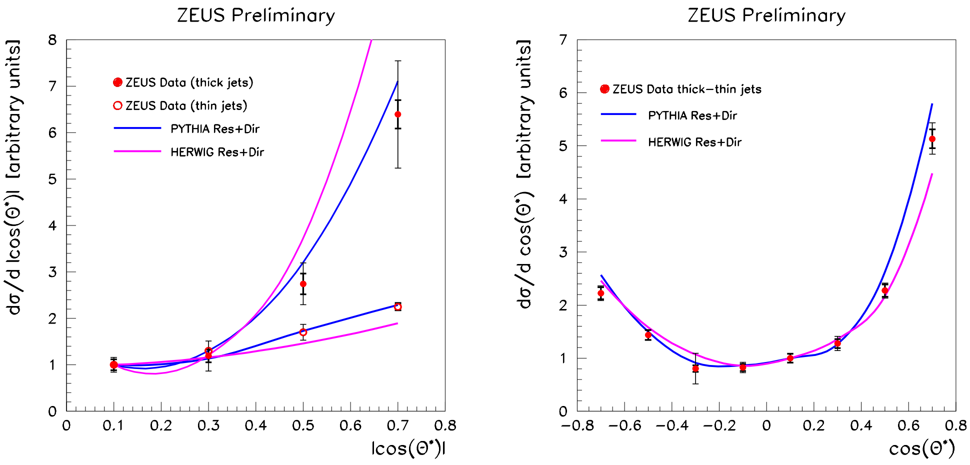

Figure 9: ZEUS preliminary jet cross-sections versus $\cos\theta^*$ compared to HERWIG and PYTHIA.

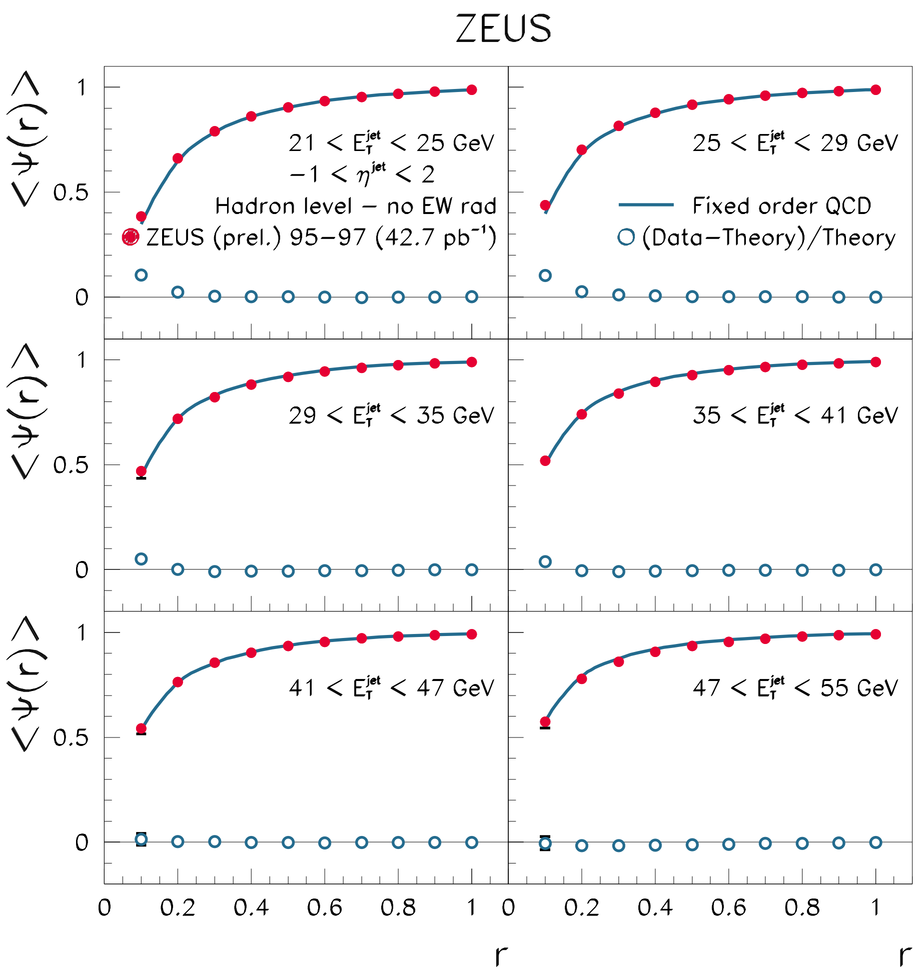

Figure 10: ZEUS preliminary data on the mean jet-shape compared to $\mathcal{O}(\alpha_s^2)$ QCD for different jet transverse energies.

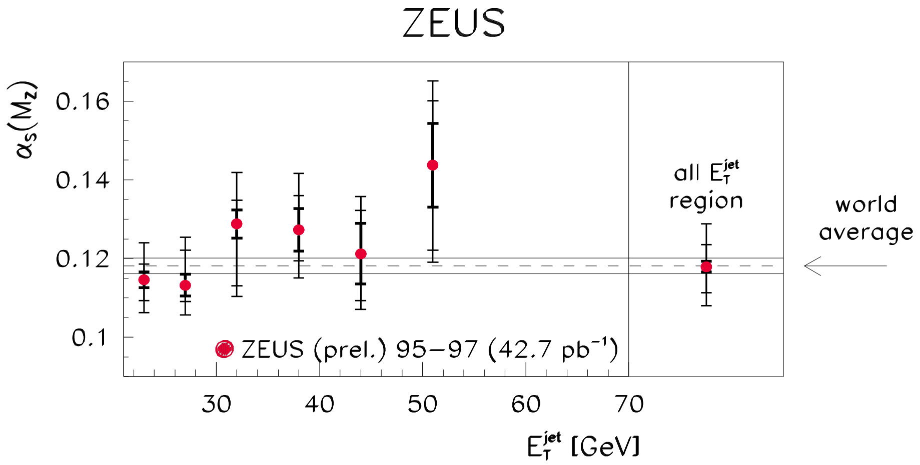

Figure 11: ZEUS preliminary values of α_S extracted from the jet-shape data.

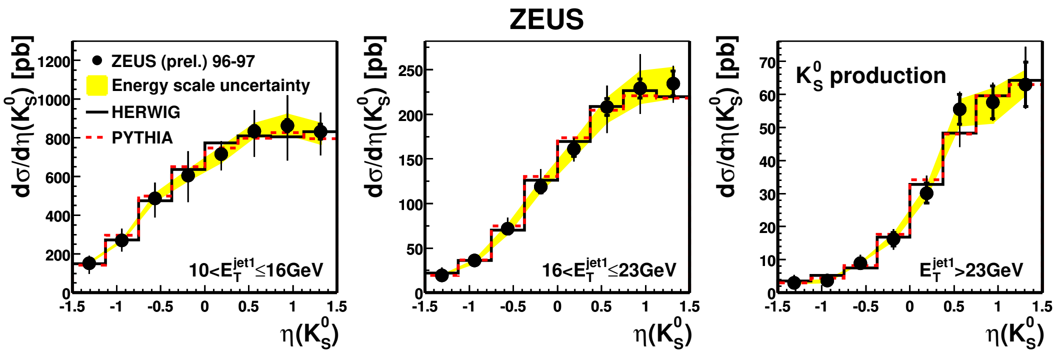

Figure 12: ZEUS preliminary cross-sections on K_S^0 meson production versus the meson pseudo-rapidity for high transverse energy dijet photoproduction.

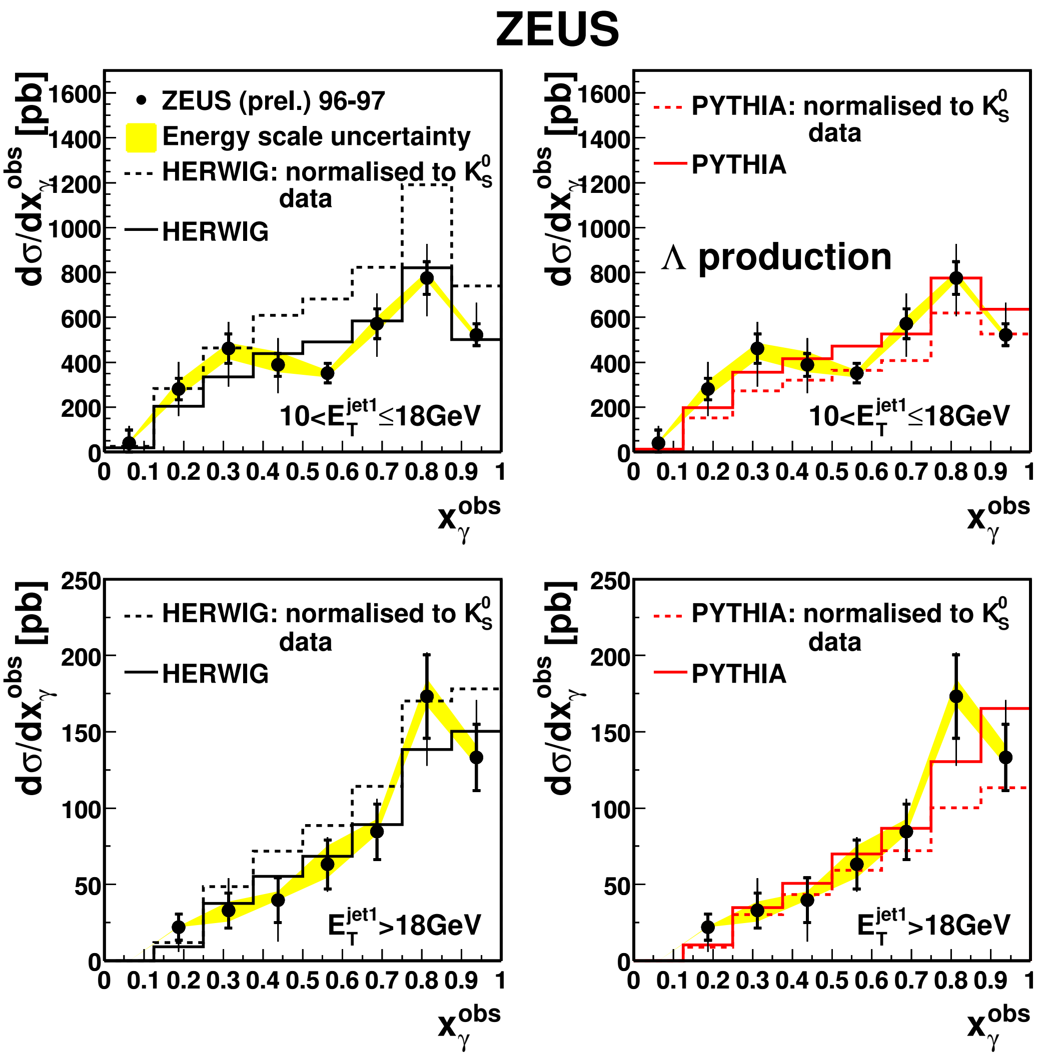

Figure 13: ZEUS preliminary preliminary cross-sections on Λ production for high transverse energy dijet photoproduction normalised both to the Λ data (solid) and to the K_S^0 data (dashed).

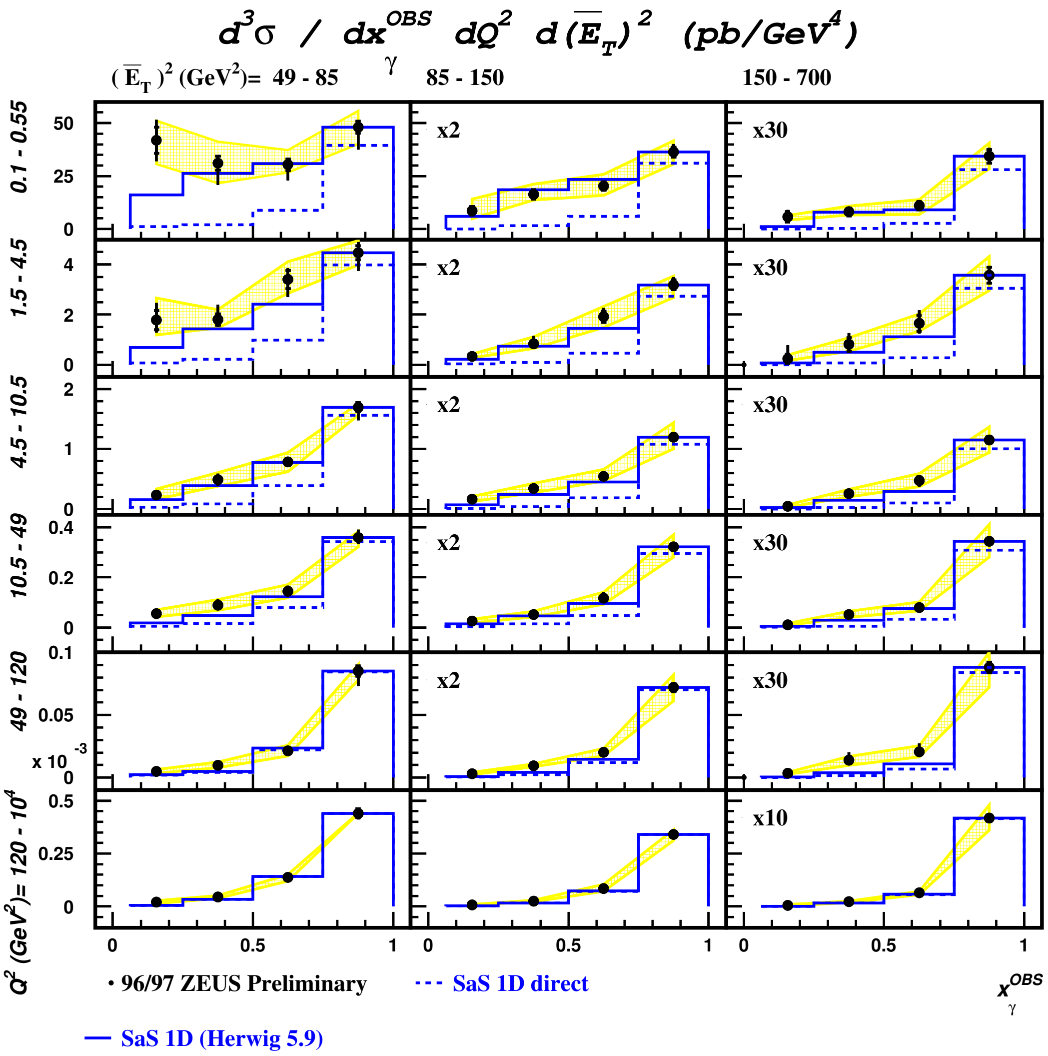

Figure 14: ZEUS preliminary dijet cross-sections, triply differential in Q^2, mean jet transverse energy squared and $x_\gamma^{\rm OBS}$ compared to HERWIG.

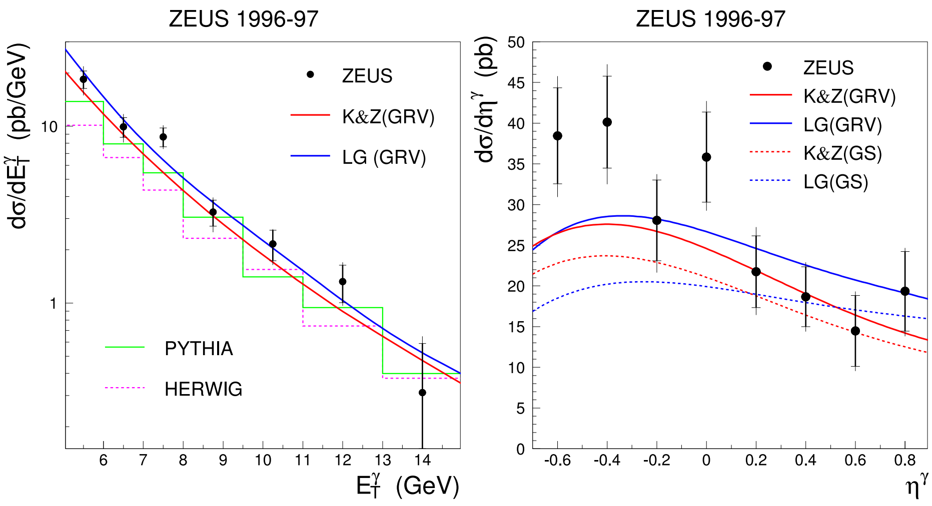

Figure 15: (a) E_T distribution of prompt photons in ZEUS (left plot), (b) pseudorapidity distribution (right plot).